Reports

Heat Production by Sediment: Ecological Significance

Abstract. *Sediments held at constant temperature evolve heat at rates that can be measured by direct calorimetry. The heat production rates decrease with depth from the surface layer. Total heat flux is an indication of the rate of degradation of potential chemical energy originally fixed by photosynthesis and represents benthic energy flow.*

A conceptual model of chemical energy storage, transfer, and transformation in the sediment and across the sediment-water interface shows that there is an equivalent rate of heat production for each biological and chemical process taking place (*1*). The total heat flux from the sediment, excluding heat flow caused by solar heating, should represent the rate of the combined processes, including metabolic transformations and extracellular chemical reactions. The rate of heat production by sediments held at constant temperature can be measured by direct calorimetry (*2*) with a double-twin heat flow calorimeter (*3*).

The term energy flow, as used in ecology, is the energy equivalent of organic matter that is ingested by living organisms less what is egested or not assimilated. It includes respiratory heat loss and energy storage in somatic tissues, gonads, fatty deposits, and so on. The concept is reasonable because of the temporary nature of stored energy, which is ultimately converted into heat. Direct calorimetry measures the continuous conversion of chemical energy into heat. Some of the original energy bound in organic matter may be converted to inorganic form in sediments; sulfides, which are reoxidized back to sulfate through direct oxidation, are an example of such a process. The heat evolved by the reaction originates from bound energy of organic matter that was oxidized by the sulfate-reducing bacteria that produced the sulfides. By this line of reasoning, the entire heat production by sediments may be equivalent to the oxidation of organic matter, of which an unknown fraction is oxidized through respiratory processes.

Direct calorimetry has the advantage over other techniques for measuring metabolic rates because all metabolic types produce heat, and the heat has unidirectional flow and dissipates without recycling. The amount of heat produced, or rate of heat production, by one organism is directly comparable to that of any other organism. The technique is especially useful with sediments that contain mixed communities of anaerobes, fermenters, and aerobes, because the total metabolic activity of such communities can be measured. Other techniques either (i) deal with a specific metabolic type or with microorganisms but not meiofauna, macrofauna, and so forth; (ii) measure a rate of production of metabolic by-product that is recycled at unknown rates; or (iii) measure a rate of uptake of an added organic substrate (without revealing its metabolic fate) from an unknown fraction of the community and require mixing, shaking, or stirring. The activity of the electron transport system of organisms that possess a respiratory chain can be determined enzymatically (*4*), but the technique runs into analytical difficulty when applied to reduced sediments, is biased against fermenters, and the results cannot be easily converted to natural rates (*2*). The use of tracer techniques allows accurate measurement of natural rates of, for example, sulfate reduction (*5*). Such specific methods are needed to evaluate the relative importance of organisms in community metabolism. If the results are accurately converted to their enthalpy equivalents, the sum should agree with the integrated measure by direct calorimetry less the heat of extracellular chemical reactions.

To sample a mud flat during low water, a petri dish (8.5 cm in diameter and 1 cm deep) is inverted over the sediment surface. The enclosed air is vented out through fine capillary tubing while the dish is pushed down and completely filled. It is dug out, the excess sediment sliced off, and the layer transferred into a similar petri dish so that the original sediment surface is exposed. Unavoidable edge disturbance takes place during the transfer, but in less than an hour the surface looks as it did before: benthic diatoms spread out over the surface, amphipods go in and out of their tubes and burrows, and overall the behavior of the captured organisms appears normal. The sample layer is placed in a metal canister (0.5 liter), and bay water is slowly siphoned in until the sediment surface is just covered. The canister is sealed airtight with a double layer of oversize rubber bands. Oxygen in the enclosed air diffuses through the thin layer of water to keep the sediment surface oxygenated, and there is enough oxygen to keep the sample aerobic for days.

When sampling subsurface layers (during tidal exposure) the overlying layer is scraped off and the desired sample is taken as before. Anaerobic samples consist of two dishes filled with sediment from the same layer which are placed face to face; the edges are then sealed with a rubber band. All anaerobic samples therefore contain twice the sediment volume as aerobic. The momentary exposure of reduced sediment to oxygen appears to be inconsequential. The hermetically sealed glass container is placed inside the metal chamber that is flooded with water which simply conducts the heat.

Typical thermograms at 20°C for surface and subsurface sediments from Corte Madera mud flat in San Francisco Bay (field temperatures fluctuated around 20°C) are shown in Fig. 1. Samples were pre-equilibrated in an antechamber before being placed in the calorimeter, but after opening the instrument at room temperature and placing the sample inside it still took 6 to 7 hours before thermal equilibrium was established. Thermogram fluctuations result from changes in heat flow and not from thermal noise.

Figure 1A shows the thermogram produced by a water sample in which a 4000-ohm resistor is immersed. When put in place the resistor had 3.00 V across it to produce a steady power of 2.25×10^{-3} J sec^{-1}. When the power was turned off, thermopile voltage dropped by 85 μV to give the calorimeter constant 2.65×10^{-5} J sec^{-1} μV^{-1}. Note that the baseline is not zero. From the time before this sample was introduced until the 26th hour, the baseline had drifted continuously by 3 μV. Baseline drift is continuously monitored by the other twin side of the calorimeter, and corrections for drift are made accordingly.

0036-8075/82/0122-0395$01.00/0

Table 1. Heat production rates of sediment from a San Francisco Bay mud flat under different experimental conditions in November 1980.

Sediment layer (cm)	Amount of sediment		Heat production (J $hour^{-1}$)		
	Volume (cm^3)	Dry weight (g)	Anaerobic*	Aerobic†	Aerobic‡
0 to 1	115	55.3	9.28	13.4	4.20
1 to 2	115	67.5	2.30		
2 to 3	115	81.9	2.02		
3 to 4	115	81.8	1.33		
4 to 5	115	93.0	1.44		
5 to 6	115		1.10§		
6 to 7	115	91.23	0.76		
0 to 7	805		18.2	22.3	

*Represents anaerobic metabolism (including fermentation) + extracellular chemical reactions. †Sediment surface is exposed to dissolved oxygen in water that is in contact with air. Total heat production represents aerobic + anaerobic + fermentation + chemical oxidation + other extracellular chemical reactions. Differences between values in the anaerobic and this column should be an estimate of aerobic respiration + chemical oxidation (4.1 J $hour^{-1}$). ‡Material retained in a 0.14-mm screen from identical volume of sediment that gave results in the preceding two columns. Value should represent aerobic metabolism of all included organisms. Compare this value with that obtained from the difference between the preceding two columns (4.1 J $hour^{-1}$). §Interpolated value between the 4- to 5-cm and 6- to 7-cm layers.

The anaerobic layers (1 to 2 cm and deeper) produced heat at fairly steady rates that decreased with depth (Fig. 1, C to G). Samples from a depth of 10 to 11 cm at different seasons produced no measurable heat. The anaerobic layer from 0 to 1 cm (Fig. 1B) produced the highest initial rate which decreased exponentially with time; by the end of 16 days the rate of heat production was down to 5 percent of peak rate (9.28 J $hour^{-1}$ for the entire sample, or 0.17 J $hour^{-1}$ per gram of dry sediment). The observed death of meiofauna in a replicate sealed sample over 3 weeks points to progressive decline in facultative anaerobic metabolism as the main cause of decrease in heat flow.

The rate of heat production of the aerobic layer (0 to 1 cm) decreased with time (Fig. 1C). This particular sample was flooded with water more than 1 cm deep. When similar samples were either exposed to air or just barely covered with water their thermograms leveled off and remained stable from hour 6 on. Evidently, a relatively thick layer of overlying water slowed the transfer of oxygen to the sediment enough to diminish the rate of aerobic metabolism. Note that in order for this aerobic sample to be comparable with the anaerobic samples, the thermogram values should be doubled. The thermopile voltage on hour 6 (70 μV × 2) gives the closest estimate of this layer's natural heat production rate.

Two replicate samples from the 0 to 1 cm layer were swirled through a 0.14-mm sieve, which retained some sediment, mostly fecal pellets, nematodes, polychaetes, ostracods, harpacticoids, amphipods, and others of minor taxonomic groups. Everything collected on the sieve was placed in a metal canister with about 100 ml of aerated bay water. This sample showed a cyclic fluctuation in heat production (Fig. 1B) probably due to the periodic swimming activity of some species. The upward trend in the thermogram might represent increasing bacterial growth. Because of the unnatural state of this sample, measurements yield only a rough estimate of total metazoan plus some microbial metabolism and their relative contribution to total heat production. The difference between the peak voltage of the anaerobic layer from 0 to 1 cm (97 μV, 6 hours after time zero) and the voltage at 6 hours of the aerobic layer from 0 to 1 cm (70 μV × 2 for a comparable sediment quantity or 140 μV) represents aerobic respiration plus chemical oxidation (4.1 J $hour^{-1}$). Note that anaerobic heat flow (9.28 J $hour^{-1}$) includes the metabolism of facultative anaerobes that were aerobic in the presence of oxygen.

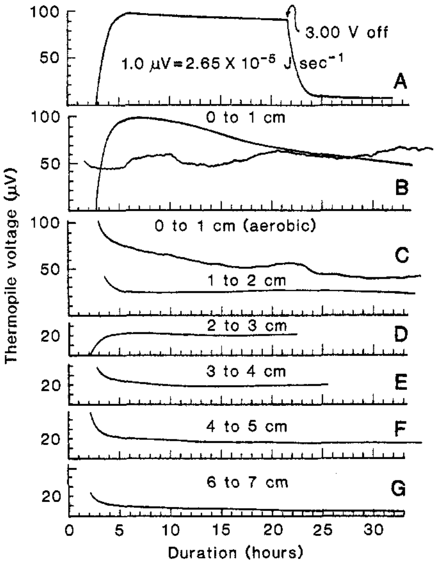

Fig. 1. Continuous recordings of calorimeter signal output from samples from different depths held at 20°C. One sample per day was taken during low water on a mud flat in northern San Francisco Bay until all layers had been measured. (A) Seawater (200 ml) in which a 4000-ohm resistor was immersed with 3.00 V across it when the sample was put in. (B) Anaerobic sediment (115 cm^3) from layer at 0 to 1 cm (smooth curve); material retained on a 0.14-mm sieve (all organisms plus some sediment) from a 115-cm^3 sample of the layer at 0 to 1 cm in unstirred aerobic water in equilibrium with enclosed air (fluctuating curve). (C) A layer at 0 to 1 cm (55 cm^3) submerged in unstirred water in equilibrium with enclosed air (top curve); 115 cm^3 of an anaerobic 1- to 2-cm layer (bottom curve). (D to G) Samples of anaerobic sediment (115 cm^3 each) from the layers indicated.

The equivalent heat production rates calculated from the thermograms are summarized in Table 1. The total heat production rate for the 7-cm column equals 18.2 J $hour^{-1}$; the sediment column's cross-sectional area is 113 cm^2 (twice that of a single petri dish), and its heat production per square meter is 1600 J $hour^{-1}$. This represents anaerobic metabolism plus heat effects of all possible extracellular chemical reactions. With the layer from 0 to 1 cm exposed to dissolved oxygen, the integrated sediment column heat production equals 22.3 J $hour^{-1}$; this is equivalent to 1960 J $hour^{-1}$ m^{-2}. This value is an estimate of the actual energy flow from the mud flat at the time of sampling. Benthic community metabolism has commonly been estimated from measurements of oxygen consumption (*6*). Simultaneous measurements of heat production and oxygen uptake [converted by Ivlev's oxycalorific coefficient in (*6*)] showed that rates of surface oxygen uptake by Corte Madera sediment are 25 to 30 percent less than actual heat production rates, the difference presumably representing subsurface anaerobic metabolism. However, the use of Ivlev's conversion factor is questionable because sediment oxygen uptake is not only by aerobic respiration. As a matter of general interest, heat flow rates may also be compared with the solar constant (4.87 × 10^6 J $hour^{-1}$ m^{-2}, the solar radiation entering the earth's atmosphere) and the heat flux from the deeper parts of the earth measured in the oceans [mean of 3718 measurements = 287 J $hour^{-1}$ m^{-2} (*7*)].

The value in the last column in Table 1 (4.2 J $hour^{-1}$) represents the aerobic metabolism of all organisms retained in a 0.14-mm sieve. One would expect a value for total aerobic metabolism to be less than that of the sum of aerobic respiration plus chemical oxidation (4.1 J $hour^{-1}$). The seemingly close agreement between the two independent estimates is probably by chance and indicates that there are problems of measurement. One problem is that infauna removed from sediment (although the organisms in this experiment were in sediment equal to 12 percent of the original amount) respire at a higher rate than those in natural sediment, especially when densely packed together (*8*). Their true undisturbed aerobic respiration is probably closer to half the rate shown in this experiment.

The amount of heat produced and rate of heat production by sediments are clearly insignificant in the total heat budget of the mud flat; that is, in comparison with the daily solar heating, nighttime cooling, and tidal heat transport. The heat itself is of no apparent ecological consequence. It is our eventual understanding of the processes that generate this heat that is important in ecology.

MARIO M. PAMATMAT
Tiburon Center for Environmental Studies, San Francisco State University, Tiburon, California 94920

References and Notes

1. M. M. Pamatmat, *Limnol. Oceanogr.* **16**, 536 (1971).
2. ——, G. Graf, W. Bengtsson, C. S. Novak, *Mar. Ecol. Prog. Ser.* **4**, 135 (1981).
3. M. M. Pamatmat, *Mar. Biol.* **53**, 223 (1979).
4. F. P. Christensen and T. T. Packard, *Limnol. Oceanogr.* **24**, 576 (1979).
5. B. B. Jorgensen, *ibid.* **22**, 814 (1977); R. W. Howarth and J. M. Teal, *ibid.* **24**, 999 (1979).
6. M. M. Pamatmat, in *Ecology of Marine Benthos*, B. C. Coull, Ed. (Univ. of South Carolina Press, Columbia, 1977), p. 89. Oxygen consumption is commonly converted to heat production by use of the average value of 20.1 J · ml^{-1} O$_2$ [V. S. Ivlev, *Biochem Z.* **275**, 49 (1934)].
7. R. Haenel, in *Terrestrial Heat Flow in Europe*, V. Cermak and L. Rybach, Ed. (Springer-Verlag, Berlin, 1979), p. 49.
8. M. M. Pamatmat, in *The Dynamic Environment of the Ocean Floor*, K. A. Fanning and F. Manheim, Eds. (Heath, Lexington, Mass., in press); W. B. Vernberg, B. C. Coull, D. D. Jorgensen, *J. Fish. Res. Board Can.* **34**, 164 (1977).
9. Supported by NSF grant OCE-8003197 and by the U.S. Geological Survey, Branch of Pacific-Arctic Marine Geology, Menlo Park, Calif. I thank R. H. Nichols and J. Conomos for their support and C. O. Davis for his critical reading of the manuscript. Contribution No. 2 of the Tiburon Center for Environmental Studies.

3 February 1981; 28 September 1981

Visibility of Comet Nuclei

Abstract. *Photography of the nucleus of comet Halley is the goal of several planned space missions. The nucleus of a comet is surrounded by a cloud of dust particles. If this cloud is optically thick, it will prevent observation of the nuclear surface. Broadband photometry of nine comets has been analyzed to determine the visibility of their nuclei. Only in the case of comet West near perihelion was the dust dense enough to interfere with imaging. Comparison of the visual brightness of the well-observed comets with that of Halley in 1910 leads to the conclusion that the nucleus of Halley can be imaged without significant obscuration by the dust.*

A number of international efforts are in the planning stage for the study of comet Halley, which is expected to reach perihelion in February 1986. Space missions could carry cameras close enough to photograph the nucleus of this comet. However, it is not clear that the dust coma will be optically thin enough to reveal the nucleus. Direct observation of the nucleus is important since it can distinguish between the generally accepted view that the nucleus of a comet is a mixture of ices and dust, as originally suggested by Whipple (*1*), and a minority view espoused by Lyttleton (*2*), that there is no nucleus, only a swarm of particles. In the Whipple model the gas produced by the sublimation of ices carries the dust grains away from the nucleus to produce the coma and dust tail. The sublimation of cometary ice is not likely to be uniform over the surface, and spacecraft imagery may reveal active areas or "jets" that are responsible for the nongravitational forces on comets (*3*). It is shown here that broadband infrared and visual observations can be used to obtain useful estimates of the optical depth τ of the dust shell without extensive modeling of the dust or coma.

Broadband observations over the wavelength, λ, range from 0.5 to 18 μm have been obtained for nine comets during the last decade. These data may be used to calculate the optical depth of the dust in the comae of these comets. Consider the case of comet West. Figure 1 shows the power distribution for comet West on 24.8 February 1976. The short-wavelength radiation is primarily scattered sunlight, and the long-wave radiation is thermal radiation from the dust grains. The short-wave data are fit by a 6000 K blackbody appropriate for the scattered sunlight; the long-wave data can be represented by a 880 K blackbody with a superimposed silicate excess. This 10-μm excess is due to the presence of small silicate grains of radius approximately 1 μm (*4*). In Fig. 1 log λF_λ is plotted against log λ. For a blackbody on such a plot, the power flux is given by $F = 1.36\ (\lambda F_\lambda)_{\max}$ W/cm^2. In the case of comet West, the energy received in the visual is 2.58×10^{-12} W/cm^2 and in the infrared is 5.44×10^{-12} W/cm^2. The ratio of the energy in the visual to that in the infrared is 0.47, and the albedo at this scattering angle is 0.47/1.47 = 0.32. The comet dust shows strong forward scattering and the bolometric Bond albedo for comet West is between 0.3 and 0.5 (*5*).

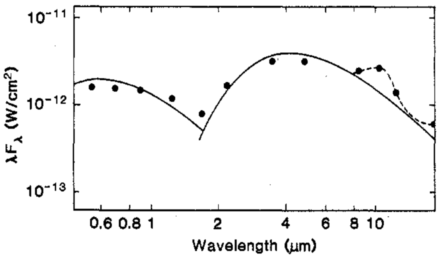

Fig. 1. Observed power distribution of comet West on 24.8 February 1976.

The long-wave thermal emission is from small grains, for which the infrared emission efficiency is proportional to their radius. As a consequence, the infrared luminosity depends on the mass of the grains in the observed geometry and is independent of particle size. The relation between emission efficiency, grain radius, and temperature depends on the optical properties of the grain material. An expression for the total observed grain mass has been derived (*6*) and is given by

$$M = 1.7 \times 10^{35} \frac{(\lambda F_\lambda)_{\max} \Delta^2}{T^4} \qquad (1)$$

where $(\lambda F_\lambda)_{\max}$ is the infrared value in watts per square centimeter, Δ is the earth-comet distance in astronomical units (1 AU = 1.5×10^8 km), and T is the grain temperature in kelvins. Using $T = 880$ K, $(\lambda F_\lambda)_{\max} = 4 \times 10^{-12}$ W/cm^2; and $\Delta = 0.85$ AU leads to a mass of 9.6×10^{11} g. The mass loss rate may be obtained by dividing the mass by the residence time, or the time for a dust grain to travel a linear distance determined by the angular radius of the observing diaphragm, which is 10 arc seconds in this case. The velocity of the dust leaving the nucleus is approximately sonic in the gas, or about 0.5 km/sec (*7*). The residence time is therefore approximately 10^4 seconds and the mass loss rate 7×10^7 g/sec. The optical depth produced by the outflowing dust can be estimated from detailed models, which must make assumptions about the grain size distribution and the optical properties of the dust.

There is, however, a more direct approach to determining the optical depth. It has been demonstrated by observations with diaphragms of radius 5 arc seconds to 1 arc minute that the value of $(\lambda F_\lambda)_{\max}$ is proportional to diaphragm radius (*8–10*). This is expected for dust that leaves the nucleus at a fixed velocity and subsequently satisfies the continuity equation (the dust flows freely with no creation or annihilation of the grains).

0036-8075/82/0122-0397$01.00/0 Copyright © 1982 AAAS